Secondary mineralization processes in pyroclastic rocks of Surtsey, Iceland (ICDP-Sustain Project)

Giovanna Montesano

Department of Earth, Environment and Resource Sciences, University of Napoli - Federico II, Via Cintia 26, 80126, Napoli
DOI: 10.19276/plinius.2025.01.014

INTRODUCTION AND SCIENTIFIC OBJECTIVES

Surtsey is the youngest and the southernmost island of the Vestmannaeyjar archipelago, which marks the seaward extension of Iceland's East Volcanic Zone. First emerging from the ocean surface in 1963, Surtsey was subsequently built up through the interplay of phreatomagmatic and effusive volcanism until 1967. Since it emerged, Surtsey immediately aroused interest among scientists to investigate the formation of a new volcanic island from the very beginning, but only a limited number of them have been permitted to access the island, and, while the eruption was still going on, it has been declared a natural reserve. Consequently, the island is a pristine geological research laboratory. The scientific value of Surtsey was further acknowledged after it became evident that the island would persist, thus providing an exceptional opportunity to study the development of an oceanic island from its origin on the sea floor to the modification of the newly erected structure by hydrothermal processes and wave abrasion. Finally, in 2008, Surtsey was designated a UNESCO World Heritage site. Investigations about the structure and stratigraphy of the volcano, nature of its hydrothermal system, notably thermal conditions, and nature of basaltic tephra hydrothermal alteration and authigenic mineral growth were first carried out in 1979 by a 181-m-deep cored drill hole. During the summer of 2017, three new cores were drilled on the island during the Surtsey Underwater volcanic System for Thermophiles, Alteration processes and Innovative Concretes (SUSTAIN) project, sponsored by the International Continental Drilling Program (ICDP) and funded by several Universities and Research Institutions. The SUSTAIN drilling program was born to sample tephra deposits through a neo volcanic island from the surface to the seafloor, with all the precautions taken to avoid contamination from the surroundings, designating samples as collaborative materials for interdisciplinary research, to trace geological and biological history of Surtsey deposits, the consolidation of freshly erupted tephra and the lithification of the lapilli tuff that currently make up the island. This study aims to investigate hydrothermal water-rock interaction, glass alteration, authigenic and secondary phases formation, taking into account subaerial and submarine samples retrieved during the SUSTAIN program through the volcanic structure of Surtur, the eastern cone of Surtsey island. The samples analyzed in this study come from the three new cores drilled in 2017 in the frame of the SUSTAIN project. All samples were investigated through optical microscopy (OM), X-Ray Powder Diffraction (XRPD) and Field Emission Scanning Electron Microscopy coupled with an Energy Dispersive Spectroscopy (FESEM-EDS), performed at the Department of Earth, Environmental and Resource Sciences (DiSTAR) of the University of Napoli Federico II (Italy). Clay minerals identification was performed at the Institute of Geological Sciences, Polish Academy of Science (Instytut Nauk Geologicznych, Polskiej Akademii Nauk – ING PAN, Kraków, Poland) on representative samples through a clay-fraction separation. Single-crystal analysis was performed on representative samples at the ID15B beamline of the European Synchrotron Radiation Facility (ESRF) in Grenoble (France). The integration of different analytical techniques to describe the suite of samples is pivotal to evaluate the mineralogy and crystal chemistry of authigenic and secondary phases, providing valuable information about their stratigraphic distribution within the subaerial and submarine volcanic structure of Surtur, as well as their paragenetic relationships with glass. Furthermore, this Ph.D. research project represents the first detailed comprehensive petrographic, mineralogical and chemical characterization of primary minerals, authigenic (*i.e.*, palagonite and clay minerals) and secondary (*i.e.*, calcium and aluminium silicates) in Surtsey samples from all the recent 2017 drill cores.

SURTSEY

Named from the name of the giant Surtr, from Norse mythology, and ey (*i.e.*, island), Surtsey Island has become one of the best-monitored volcanic sites on Earth.

Its eruption is the typical example of shallow-to-emergent subaqueous explosive volcanism, demonstrating how magma-water interaction affects fragmentation dynamics to create typical steam-rich tephra jets and fine-grained deposits. Its growth has been thoroughly chronicled by a nearly continuous record of observations, contributing to make it the type example of pyroclastic activity, now recognized as Surtseyan volcanism (Schipper et al., 2015). The Surtsey volcano (Fig. 1) is located in the southernmost sector of the Vestmannaeyjar archipelago, which forms the offshore extension of the Iceland SE rift zone. The island grew from a seafloor depth of ~ 130 m during explosive and effusive basaltic eruptions in 1963–1967 and represents the subaerial portion of the whole Surtsey volcano, which forms a northeast to southwest oriented, mainly submarine ridge approximately 5.8 km long (Jakobsson & Moore, 1986). The main topographical features of Surtsey island are two crescent-shaped cones of tephra and palagonite tuff (Fig. 1), covering an area of 0.72 km^2, named Surtungur (or also Surtur I or Austurbunki) and Surtur (or also Surtur II or Vesturbunki), along with a lava field that caps the southern half of the island. The eastern cone (Surtur) rises to an elevation of 155 m and displays several small lava craters and fissures, whereas the western cone (Surtungur), with a height of 141 m, exhibits slump scars on its western side due to marine abrasion. The constant modification of Surtsey shape is attributed to the challenging weather conditions prevailing in the sea south of Iceland, particularly during the winter season.

Surtsey hydrothermal system, thermal field and palagonitization of Surtsey deposits

Long-term monitoring and mapping have been conducted on the hydrothermal system of Surtsey volcano to gain insight into the rate at which tephra transformed into palagonite tuff, reinforcing volcanic structures and thus enhancing slope stability and fortification against erosion. The first signs of hydrothermal activity, consisting of a zone of anomalous heat exchange, were observed on the island close to the newest lava craters erupted during January 1967 as visible steam rising from the tephra pile (Friedman & Williams, 1970). Since that time, detailed studies have been conducted on the origin and nature of the hydrothermal system in the volcano, as well as the process of tephra alteration, with a thermal survey performed on average every three years (Jakobsson et al., 2000). Evidence from a 181 m-deep drill hole (named SE-01) conducted at Surtsey in 1979 (Fig. 1c) indicates that the heat in the hydrothermal system was most likely generated by the basaltic intrusion that fed the lava flows from 1964 to 1967, which occurred both above and below the sea level at Surtur and Surtungur (Stefánsson et al., 1985). The first temperature measurements were conducted by Jakobsson S.P. in September 1969. He used a traditional mercury thermometer placed at about 5 cm depth in the hottest area of the Surtur vent, where steam was escaping and recorded surficial temperature ranging from 48 to 84°C (Jakobsson, 1978). Between 1969 and 1972, surface temperatures of 40-50°C were observed in the central part of the thermal area. However, in areas with more intense steam emanations, particularly in and around lava craters, temperatures as high as 100°C were measured. This represents the highest temperature recorded on the surface of tephra (Jakobsson, 1978). The monitoring of the surface manifestations of geothermal activity served to understand the changes of the Surtsey thermal field. Overall, the data from these investigations indicate a gradual but noticeable cooling of the eruptive deposits over time (Perez, 2019).

One year after the discovery of the active hydrothermal system, the first signs of palagonitization of basaltic glass were recorded in surficial tephra at the SE of Surtur. Since then, in accordance with the thermal monitoring program established in the same year, the development of palagonite tuff has been monitored and mapped approximately every three years (Perez, 2019). During each geological survey, samples of tephra and tuff have been collected, and a detailed map of the surface of Surtsey was generated to track the growth of the thermal field and palagonite tuff (Jakobsson et al., 2000). Thus, the palagonitization process and evolution were observed in its natural environment for the first time (Jakobsson, 1978).

RESULTS

To obtain a consistent characterization of samples as a function of their depths, the six stratigraphic and hydrothermal zones of Surtur crater (McPhie et al., 2020) were followed. The samples are moderately to strongly vesicular hypo-crystalline lapilli tuffs with inequigranular grain size distributions, except the crystalline basalt (RS-33) collected from the bottom of the HOLE D drill core. In most samples, the larger clastic components, angular to slightly rounded ash- to lapilli-sized pyroclasts, and the fine ash matrix (containing loose-crystals of plagioclase both euhedral and as tiny fragments) appear extensively altered. Pyroclasts show vesicles of variable size and shape, commonly filled with authigenic minerals.

Sideromelane and primary minerals

Translucent sideromelane, pale yellowish-gray at plane-polarized light (PPL) and completely isotropic at cross-polarized light (CPL), occurs in all the hydrothermal zone deposits but not in all samples, and frequently embeds phenocrysts and microphenocrysts of plagi-

oclase and olivine (Fig. 2a-d). Although sideromelane is defined as fresh glass (Peacock & Fuller, 1928), authigenic phases (*e.g.*, clay minerals) can be present at a sub-micrometer scale, so the identification of sideromelane is based here solely on optical petrographic criteria and through FESEM-EDS analysis, not considering the potential occurrence of authigenic phases. SEM-SE images of sideromelane show a typical homogeneous, texturally uniform and smooth surface with abundant rounded, spherical to elliptical vesicles, commonly coalescent (Fig. 2a,b). By contrast, domains of altered glass display a wide range of features reflecting progressive degrees of alteration within the original vesicular morphology, shown in thin section (Fig. 2a–f).

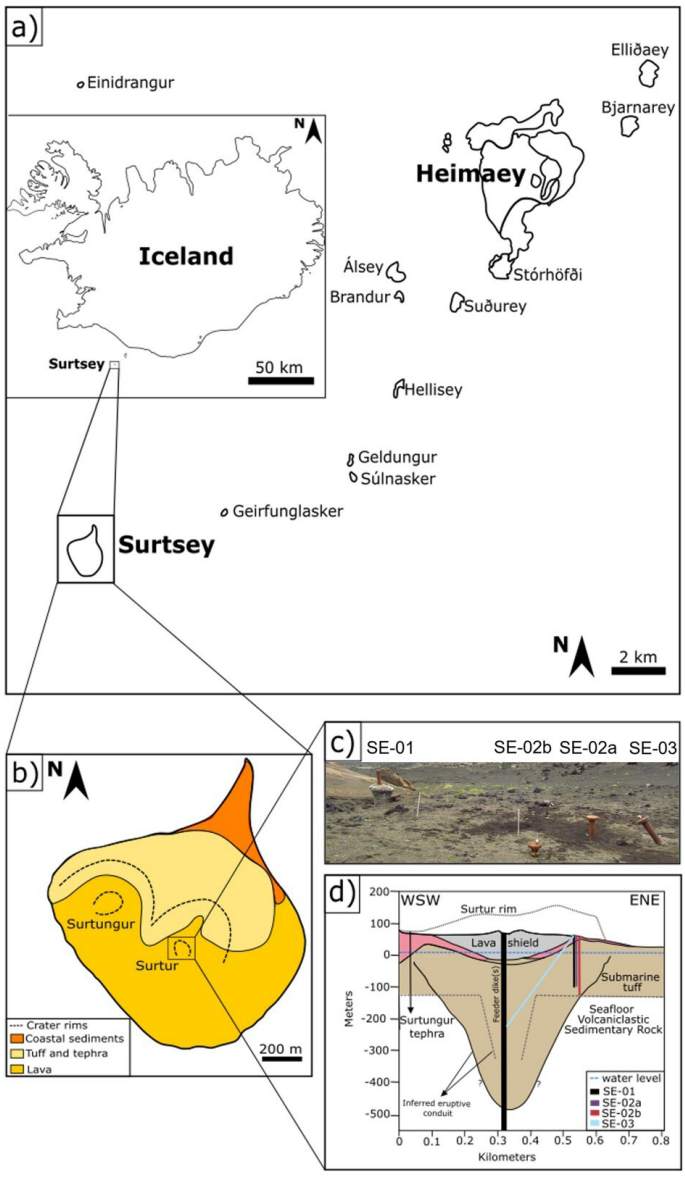

Figure 1 *Surtsey volcano, Iceland.* ***a)*** *Sketch map of the Vestmannaeyjar archipelago with Surtsey at its southwestern tip.* ***b)*** *simplified sketch map of Surtsey showing the main geo-lithological units and crater rims (dashed lines) of Surtur and Surtungur (modified after Prause et al., 2022).* ***c)*** *field photograph showing wellheads of the three 2017 and 1979 boreholes.* ***d)*** *interpretative cross-section of Surtur showing the original crater rim (at the age of its formation; dotted line), 1979 (SE-01) and 2017 (SE-02a, SE-02 b and SE-03) cored drill holes (Jackson, 2017), pyroclastic deposits, lava shield in the central crater, and seafloor volcaniclastic sedimentary rock. The subseafloor inferred eruptive conduit: black solid line (Moore, 1985) and minimum expression (gray dashed line; Jackson et al., 2017).*

Euhedral lath-shaped plagioclase and anhedral to subhedral olivine crystals (Fig. 2a–d) are ubiquitous primary phases. They occur both as phenocrysts and microphenocrysts within the altered fragments of volcanic glass and as loose crystals in the altered fine-ash matrix.

Authigenic alteration

Three principal palagonitic textures (Fig. 2a–c), as previously described by Montesano et al. (2023), are present: *i)* optically isotropic palagonitic rinds (*e.g.*, Fig. 2a), *ii)* fibrous palagonitic type (*e.g.*, Fig. 2b), and *iii)* granular, opaque palagonitic-type (e.g., Fig. 2c).

Olivine crystals can show clay-like alteration rims of variable thickness, either regular, following the original crystal boundaries, or irregular and denticulate, directed towards the interiors of the crystals. Moreover, almost complete pseudomorphic olivine replacement by clay-like secondary minerals (*e.g.*, Fig. 2d) is common. In SEM-SE images, altered basaltic glass appears in globular micro-morphological arrangements (Fig. 2e-f) or as tiny plates with curled edges or feathered "flakes" of randomly intergrown smectite-like clay minerals (Fig. 2g-h). The globules, often agglutinated, are about 3 μm in diameter. Morphological features of the altered glass are highly heterogeneous and may locally display a ragged or sponge-like surface (Fig. 2i-j), or a distinct fibrous appearance, typically with fan or leaf-shaped textures in altered olivine crystals (Fig. 2j).

Chemical composition of authigenic alteration

Regarding the chemical composition, all the investigated sideromelane analyses show a limited compositional spectrum, falling in the basalt field (SiO_2 = 45.16-48.12 wt.%). As regards alteration elements (*i.e.*, palagonitized glass and altered olivine), they show an overall lower Si, Al, Na and Ca content than sideromelane, and higher Fe and Mg. Ti content of several palagonite analyses and of most altered olivine. is lower than the Ti content of sideromelane, approaching zero.

Secondary minerals

Secondary phases occur as zeolite, calcium–aluminium–silicate hydrate, carbonate, and sulphate minerals. They are present as fillings in pyroclast vesicles and pores of the binding fine-ash matrix, as well as surface coatings in large pores of the altered ash matrix (Fig. 3): *i)* euhedral analcime typically forms coatings on the inner walls of vesicles of coarse ash or lapilli or along void spaces in the binding fine-ash matrix (Fig. 3a) and appear through SEM as euhedral and well defined crystals (3f-i); *ii)* phillipsite in vesicles appear as colourless intergrowths and radiating prismatic crystals (Fig. 3b). Phillipsite through

SEM occurs as well-defined crystals filling vesicles and displaying a rosette morphology, or replaced by analcime (3e,g-i); *iii)* tobermorite (3a-b, f, h-i) in vesicles appears as acicular microcrystals arranged in discrete fan-shapes. Tightly bound needles of Al-tobermorite also formed (Fig. 3b). Groups of randomly oriented, sprays of Al-tobermorite appear to postdate analcime and phillipsite (Fig. 3i); *iv)* highly birefringent, microcrystalline calcite forms scattered coatings along the inner walls of matrix pores (Fig. 3c); *v)* colourless, prismatic to fibrous radiating gypsum crystals (3d, j) are also present; *vi)* very few crystals of chabazite occurs as vesicle filling in association with analcime; *vii)* well-defined acicular crystals or massively bound needles associated with analcime and calcite also occur.

Chemical composition of secondary minerals

Chemical composition of secondary minerals, obtained through Energy Dispersive X-ray Spectroscopy (EDS) are the following: *i)* chabazite appears only in the shallowest zones with a Ca- and K-rich composition; *ii)* phillipsite is Ca, Na and K-rich; *iii)* analcime show an overall sodic character; *iv)* Al-tobermorite and clinotobermorite show distinct compositions, both containing Ca as prevalent cation along with K and Na, but the former also contain Al; *v)* xonotlite consists mainly of Ca and Al; *vi)* a Si-rich phase, containing almost completely Si with lesser amount of Al, Fe, Ca and alkali.

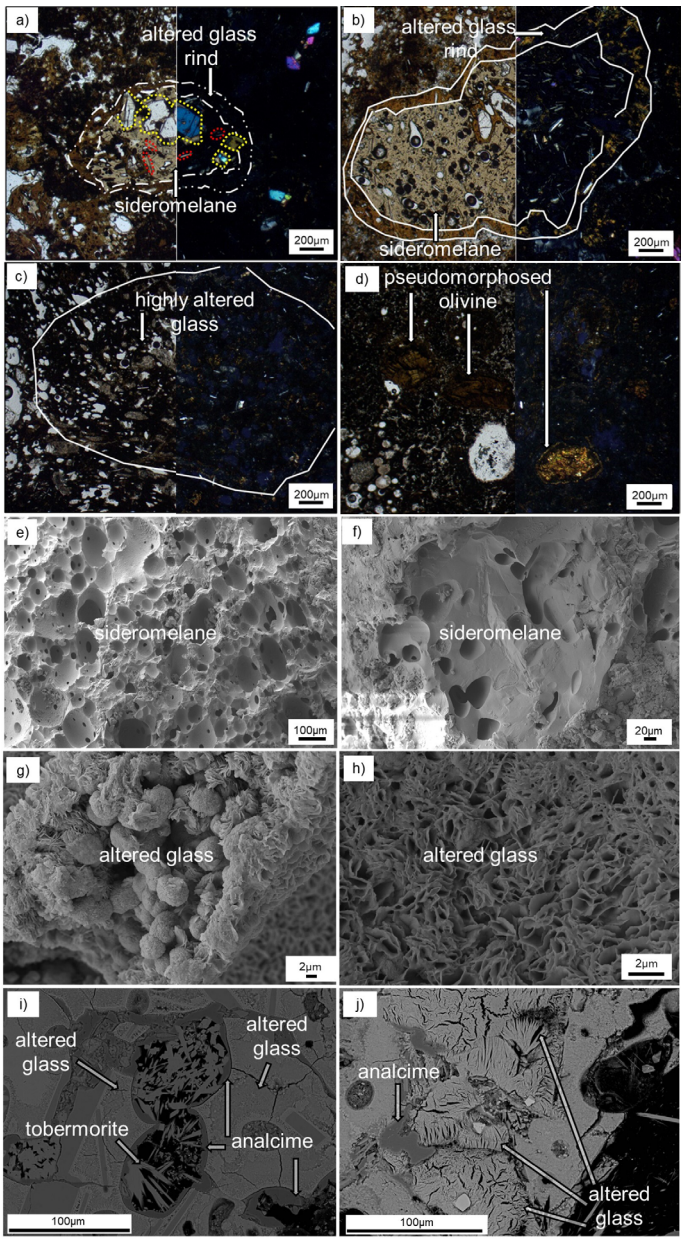

Figure 2 *Petrographic images [PPL plane-polarized light (left) and CPL cross-polarized light (right)] showing the three different types of glass fabrics:* ***a)*** *apparent sideromelane,* ***b)*** *altered glass rinds,* ***c)*** *highly altered glass and* ***d)*** *complete pseudomorphic olivine replacement by clay-like phases; SEM-SE images showing* ***e-f)*** *sideromelane;* ***g-j)*** *SEM-BSE images showing altered glass, along with tobermorite and analcime.*

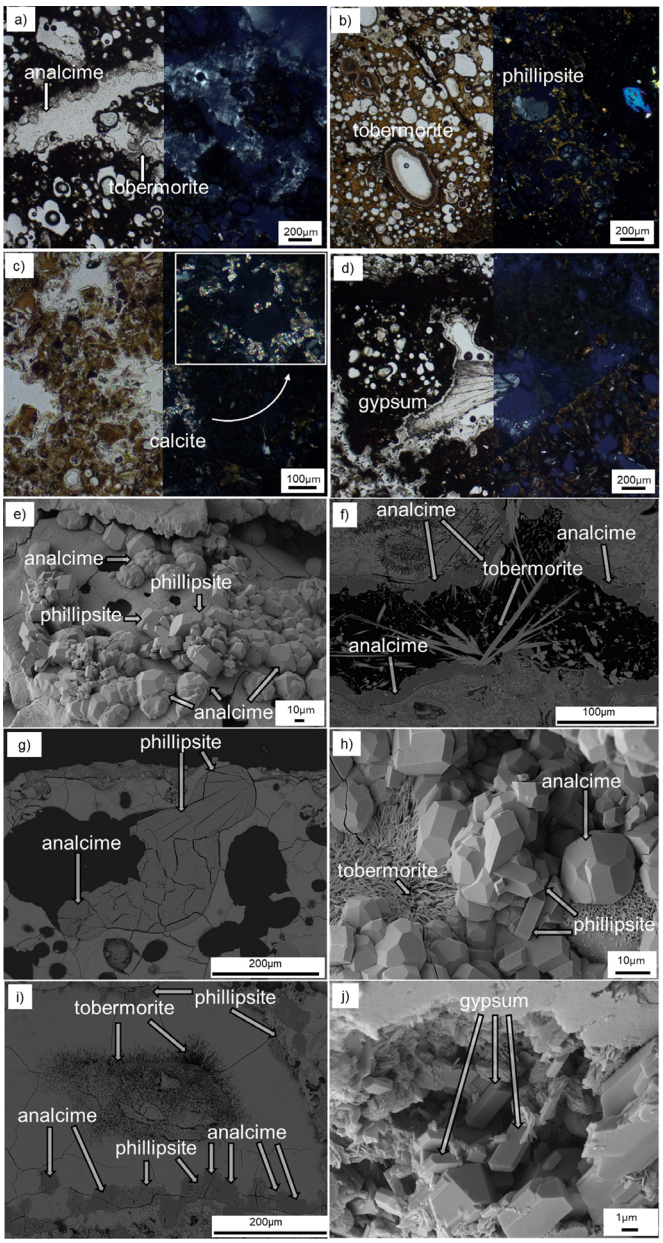

Figure 3 *Petrographic and SEM images showing secondary mineral growth.* ***a-d)*** *Petrographic images [PPL plane-polarized light (left) and CPL cross-polarized light (right)] showing* ***a)*** *analcime and tobermorite,* ***b)*** *phillipsite and tobermorite,* ***c)*** *calcite and* ***d)*** *gypsum.* ***e,h)*** *SEM-SE and* ***f,g,i)*** *SEM-BSE images showing phillipsite, analcime and tobermorite;* ***j)*** *SEM-SE image showing gypsum crystals.*

Structural characterization

Structural characterization performed through single-crystal X-ray diffraction analysis proved necessary to corroborate the presence of the very fine-grained secondary minerals. The selection of the crystals focused on pores and vesicle fillings. According to the cell parameters obtained through this analysis, the crystal selected as phillipsite to be analyzed is actually merlinoite, a rare zeolite morphologically identical to phillipsite (Gatta et al., 2015). Moreover, this analysis confirmed the presence of xonotlite, very similar to tobermorite, and also revealed the presence of a phase whose identification is still controversial.

X-Ray Powder Diffraction - mineralogical characterization of bulk samples and one-dimensional modelling of separated clay fractions

From each of the investigated rock samples, powders have been prepared for qualitative and quantitative mineralogical investigations, reported in Figure 4 and Table 1. X-ray powder diffraction analysis performed on the bulk samples detected the presence of peaks in the low-angle part of the patterns ascribable to the presence of clay minerals. For this reason, representative samples were subjected to a clay fraction separation following the procedure of Jackson (1969). The separated fractions $\phi < 0.2$ µm were acquired both at air-dried conditions (AD) and after ethylene glycol treatment (EG). The presence swelling smectites is dominant in the mineralogical assemblages of the analyzed samples, along with chlorite and serpentine (Fig. 5a). To further confirm the presence of the abovementioned phases in the separated fraction $\phi < 0.2$ µm, the acquired patterns were analyzed also through the software Sybilla (Fig. 5b), a software which help to discriminate between the various clay species (Chevron™, Zeelmaekers et al., 2007). According to the modelling through Sybilla, almost all the calculated patterns fit well with trioctahedral smectite, trioctahedral chlorite and serpentine.

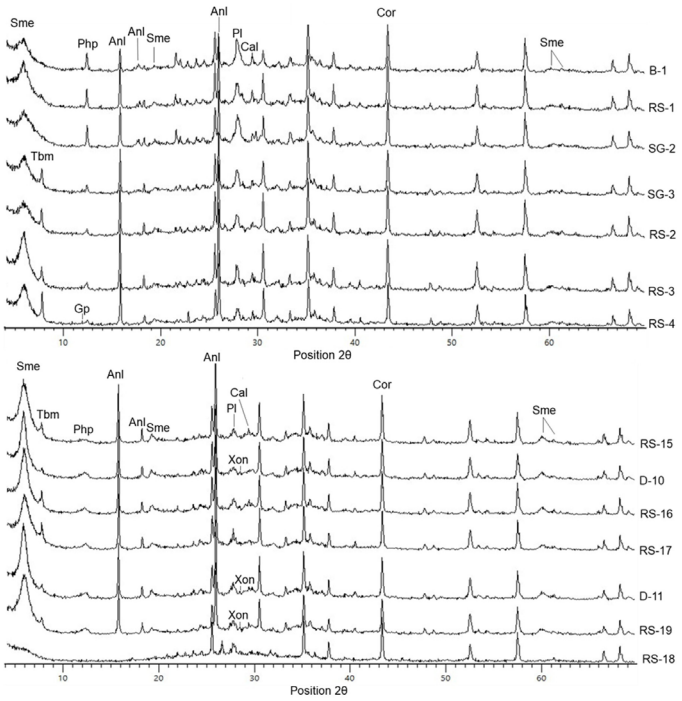

Figure 4 *Representative XRPD patterns of untreated powders of Surtsey samples.*

DISCUSSION AND CONCLUSIONS

The progressive hydrothermal alteration within the Surtsey subaerial and submarine system is recorded by two main processes: alteration of fresh basaltic glass (sideromelane) and primary minerals (mainly olivine and plagioclase), and precipitation of secondary phases as pyroclasts pores and vesicles fillings or in void spaces in the matrix. and precipitation of secondary phases as pyroclasts pores and vesicles fillings, or in void spaces in the matrix.

The presence of clinopyroxene can be explained by embracing the "pyroxene paradox" hypothesis, considering clinopyroxene as present only in the

Sample	Depth (m)	Pl	Ol	Cpx	Anl	Cal	Php	Gp	Tbm	AC
RS-1	22.6	11	3	3	12	2	10	0	2	57
RS-3	43.7	11	3	4	17	2	2	1	4	56
RS-5	65.3	6	2	5	17	2	6	0	4	58
RS-6	78.2	6	1	4	17	2	6	1	5	58
RS-8	92.6	4	1	7	21	2	4	1	5	55
RS-9	101.5	5	1	7	24	2	1	1	5	54
RS-10	110.9	6	1	7	22	2	1	1	5	55
RS-12	128	4	1	8	26	2	1	1	4	53
RS-14	148.7	12	2	4	12	2	8	0	3	57
RS-17	176.1	6	2	5	17	2	6	0	4	58

Table 1 *Representative quantitative XRPD analysis.*

Abbreviations: AC: amorphous content and disordered clay minerals; pl: plagioclase; cpx; clinopyroxene; ol: olivine; php: phillipsite; anl: analcime; tbm: Al-tobermorite; cal: calcite; gp: gypsum.

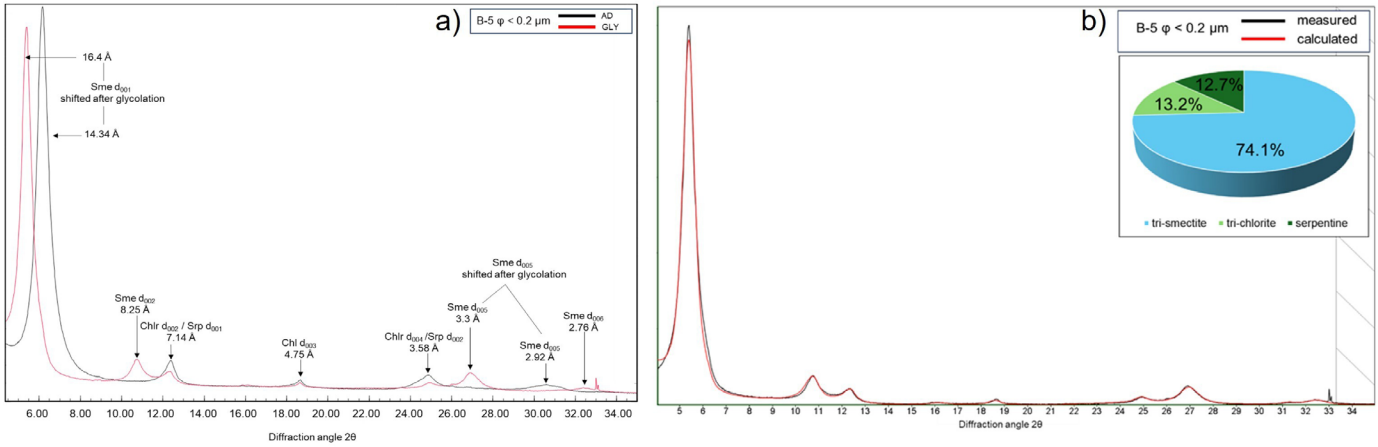

Figure 5 a) *Representative XRPD pattern of the oriented clay aggregate (ϕ < 0.2 μm) of sample B-5 acquired at air-dried conditions (AD, black line) and after ethylene-glycol solvation (EG, red line).* ***b)*** *One-dimensional modelling of EG pattern of the oriented clay aggregate (ϕ < 0.2 μm) of sample B-5. Striped areas have been excluded from modelling because they contained residual non-clay minerals. Pie chart shows the percentages of the phases used for the modelling.*

groundmass or considering that hydration reactions can lead to the transformation of pyroxene to smectite (Velbel et al., 2008). Sideromelane undergoes hydration and extensive alteration; nonetheless, significant variations in the mineralogical assemblages can be recognized in both subaerial and submarine Surtsey deposits. Different generalized temperature domains can be recognized in the Surtsey deposits basing on temperature measurements: *i)* a low temperature domain, in which temperature is lower than 90-100°C (0-65 m and 130-300 m b.s.), *ii)* a high-temperature domain, in which temperature is higher than 100-125°C (65-165 m b.s.), and *iii)* a thermal bulge where temperature reaches 140°C (80-145 m b.s.). Sideromelane in pyroclasts is still preserved in the low-temperature domain deposits, while it is almost completely altered in the high-temperature domain deposits. However, some sideromelane is still preserved where the temperature is higher. The results of this research suggest that the microenvironment (*i.e.*, fine-scale conditions related to direct glass-fluid interactions) may be just as influential as macroenvironment (*i.e.*, physical parameters of the system, such as temperature) in controlling the development of alteration products and each sample shows its own alteration history, with specific fluid–glass–crystal interactions, such that the fluid compositions in vesicles (or pores) change over time to form phases and to precipitate crystals with different and evolving compositions. Figure 6 shows a schematic representation of this process: the first element to undergo alteration is sideromelane, from which chemical elements are mobilized. The mobilization of some chemical elements entails, on one side, the *in situ* alteration (*i.e.*, authigenic alteration or palagonitization) of sideromelane, on the other, the precipitation of secondary phases. The maturation of palagonite entails the formation of clay phases. The comparison of patterns of the separated fractions ϕ < 0.2 μm acquired at air-dried conditions and after ethylene-glycol treatment and through the modelling by using Sybilla software (Chevron™, Zeelmaekers et al., 2007) displayed the presence of tri-octahedral smectite, tri-octahedral chlorite and serpentine.

As regards secondary phases, zeolites appear to be early alteration products in the crystallization sequence. Crystallization of phillipsite and analcime is mirrored as they correlate negatively with each other, and at higher temperatures, he more favourable crystallization of analcime strongly influences the presence of phillipsite. This is in accordance with the stability field proposed by Apps (1983), according to which phillipsite is stable at lower temperatures than analcime. However, they can form contemporaneously depending on the composition of the solution. Also, chabazite has been identified in the shallowest zones of lower temperature, in accordance with the zonation proposed by Apps (1983) for hydrothermally altered basalts from Iceland. Zeolites form before acicular tobermorite and xonotlite.

According to single-crystal diffraction experiments, the possible concomitant occurrence of merlinoite along with phillipsite can explain the extremely variable composition of Surtsey phillipsite. Structural characterization also confirmed the presence of xonotlite. The identification of the hydrated Si-rich crystals is still controversial.

The systematic petrographic, mineralogical and chemical analyses of sideromelane altered glass and secondary minerals of the 50-year-old pyroclastic deposits at Surtsey volcano recorded compositional variations that

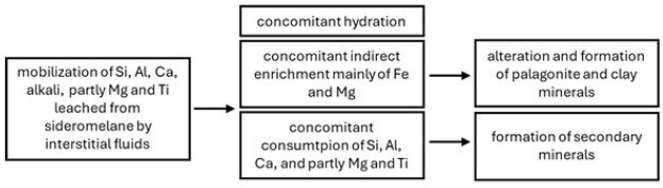

Figure 6 *Schematic explanation of authigenic and secondary phase formation in Surtsey deposits.*

provide new insights into processes that produce mineral growth in young oceanic basalts. The description of the finely resolved, spatial frameworks of mineralization in the young, active and well-monitored hydrothermal system of Surtsey volcano offers new insights into the structural organization of the alteration process and secondary mineral growth in oceanic basalt. The alteration path along the analysed subaerial and submarine sequences was identified through the integrated results, trying to develop a minerogenetic model to explain their genesis. This model would provide a reference framework for assessing the mineralogical evolution not only in other Surtseyan-type volcanoes but also in both modern and ancient different basaltic environments.

REFERENCES

Apps, J.A. (1983) - Hydrothermal evolution of repository groundwaters in basalt. In NRC Nuclear Waste Geochemistry '83, U.S. Nuclear Regulatory Commission Report NUREG/CP-0052, 14-51.

Friedman, J.D. & Williams, R.S. (1970) - Changing Patterns of Thermal Emission from Surtsey, Iceland between 1966 and 1969. U.S. Geol. Survey 700-D, 116-124.

Gatta, G.D., Rotiroti, N., Bersani, D., Bellatreccia, F., Della Ventura, G., Rizzato, S. (2015) - A multi-methodological study of the (K,Ca)-variety of the zeolite merlinoite. Mineral. Mag., 79, 1755-1767.

Jackson, M.L. (1969) - Soil chemical analysis. Advanced course. 2nd ed. published by the author. University of Wisconsin. Madison. USA.

Jackson, M.D. (2017) - Petrographic and material observations of basaltic lapilli tuff, 1979 and 2017 Surtsey drill cores, Iceland. Surtsey Res., 14, 47–62.

Jakobsson, S.P. (1978) - Environmental factors controlling the palagonitization of the Surtsey tephra, Iceland. Bull. Geol. Soc. Denmark, 27, 91–105.

Jakobsson, S.P. & Moore, J.G. (1986) - Hydrothermal minerals and alteration rates at Surtsey volcano, Iceland. Geol. Soc. Am. Bull., 97, 648–659.

Jakobsson, S.P., Guðmundsson, G., Moore, J.G. (2000) - Geological monitoring of Surtsey, Iceland, 1967-1998. Surtsey Res., 11, 99-108.

McPhie, J., White J.D.L., Gorny, C., Jackson, M.D., Guðmundsson, M. T., Couper, S. (2020) - Lithofacies from the 1963- 1967 Surtsey eruption in SUSTAIN drill cores SE-2a, SE-2b and SE-03. Surtsey Res., 14, 19-32.

Montesano, G., Rispoli, C., Petrosino, P., Jackson, M. D., Weisenberger, T.B., Guðmundsson, M.T., Cappelletti, P. (2023) - Authigenic mineralization in Surtsey basaltic tuff deposits at 50 years after eruption. Sci. Rep., 13.

Moore, J.G. (1985) - Structure and eruptive mechanism at Surtsey Volcano, Iceland. Geol. Mag., 122, 649–661.

Peacock, M.A. & Fuller, R.E. (1928) - Chlorophaeite, sideromelane, and palagonite from the Columbia River Plateau. Am. Mineral., 13, 360–382.

Perez, V. (2019) - Fifty Year Evolution of Thermal Manifestations at Surtsey Volcano 1968 - 2018, master's thesis, Faculty of Earth Science, University of Iceland, 92.

Prause, S., Weisenberger, T.B., Kleine, B.I., Monien, P., Rispoli, C., Stéfansson, A. (2022) - Alteration of basaltic glass within the Surtsey hydrothermal system, Iceland - Implication to oceanic crust seawater interaction. J. Volcanol. Geoth. Res., 429, 107581.

Schipper, C.I., Jakobsson, S.P., White, D.L., Palin, J.M., Marcinowski, T.B. (2015) - The Surtsey Magma Series. Sci. Rep., 5, 11498.

Stefánsson, V., Axelsson, G., Sigurdsson, O., Gudmundsson G., Steingrimsson, B. (1985) - Thermal condition of Surtsey. J. Geodyn., 4, 91–106.

Velbel, M.A. & Barker, W.W. (2008) - Pyroxene weathering to smectite: conventional and Cryo-field Emission Scanning Electron Microscopy, Koua Bocca ultramafic complex, Ivory Coast. Clay Miner., 56, 112-127.

Zeelmaekers, E., McCarty, D., Mystkowski, K. (2007) - 'SYBILLA user manual', Chevron proprietary software, Texas, USA.